



Since January 2020 Elsevier has created a COVID-19 resource centre with free information in English and Mandarin on the novel coronavirus COVID-19. The COVID-19 resource centre is hosted on Elsevier Connect, the company's public news and information website.

Elsevier hereby grants permission to make all its COVID-19-related research that is available on the COVID-19 resource centre - including this research content - immediately available in PubMed Central and other publicly funded repositories, such as the WHO COVID database with rights for unrestricted research re-use and analyses in any form or by any means with acknowledgement of the original source. These permissions are granted for free by Elsevier for as long as the COVID-19 resource centre remains active.



Short Communication

Ionophore antibiotic X-206 is a potent inhibitor of SARS-CoV-2 infection *in vitro*

Esben B. Svenningsen^{a,1}, Jacob Thyrested^{b,1}, Julia Blay-Cadanet^{b,1}, Han Liu^a, Shaoquan Lin^a, Jaime Moyano-Villameriel^a, David Olganier^b, Manja Idorn^b, Søren R. Paludan^b, Christian K. Holm^{b,**}, Thomas B. Poulsen^{a,*}

^a Department of Chemistry, Aarhus University, Langelandsgade 140, DK-8000, Aarhus C, Denmark

^b Department of Biomedicine, Aarhus University, Høegh-Guldbergs Gade 10, 8000, Aarhus C, Denmark



ARTICLE INFO

Keywords:

SARS-CoV-2
Coronavirus
Antiviral agent
Polyether ionophore
X-206

ABSTRACT

Pandemic spread of emerging human pathogenic viruses, such as the current SARS-CoV-2, poses both an immediate and future challenge to human health and society. Currently, effective treatment of infection with SARS-CoV-2 is limited and broad spectrum antiviral therapies to meet other emerging pandemics are absent leaving the World population largely unprotected. Here, we have identified distinct members of the family of polyether ionophore antibiotics with potent ability to inhibit SARS-CoV-2 replication and cytopathogenicity in cells. Several compounds from this class displayed more than 100-fold selectivity between viral-induced cytopathogenicity and inhibition of cell viability, however the compound X-206 displayed >500-fold selectivity and was furthermore able to inhibit viral replication even at sub-nM levels. The antiviral mechanism of the polyether ionophores is currently not understood in detail. We demonstrate, e.g. through unbiased bioactivity profiling, that their effects on the host cells differ from those of cationic amphiphiles such as hydroxychloroquine. Collectively, our data suggest that polyether ionophore antibiotics should be subject to further investigations as potential broad-spectrum antiviral agents.

The societal impact of the novel corona virus, SARS-CoV-2, that emerged in the end of 2019 (Zhu et al., 2020; Wu et al., 2020), continues to increase and the global death toll associated with the resulting respiratory disease, COVID19, is now >1.2 million. The lack of effective antiviral therapies and long hospitalizations required for patients with severe COVID19 threatens to overwhelm health care systems, which will continue to be a risk until an effective vaccine is deployed or population immunity achieved. Given the long timeframes and uncertainties involved in both of these scenarios attempts to repurpose compounds with available human safety data are of high priority (Caly et al., 2020; Touret et al., 2020; Choy et al., 2020; RECOVERY Collaborative Group, 2020). Likewise, compounds, for which animal data is available, are of strong interest for accelerated evaluation and development, in particular compounds that display broad-spectrum antiviral activity that may also be of high value beyond the current pandemic.

The polyether ionophore antibiotics is a family of natural products

with diverse biological effects (Kevin II et al., 2009; Rutkowski and Brzezinski, 2013). The compounds are most known for their inhibitory activities against gram-positive bacteria, including drug-resistant strains, and coccidian protozoa, which has led to the use of some polyether ionophores as veterinary antibiotics (Chapman et al., 2010). In addition, antiviral activities against several different families of both RNA and DNA viruses have also been documented, including HIV (Kevin II et al., 2009; Nakamura et al., 1992), influenza (Jang et al., 2018), and Zika virus (Rausch et al., 2017). Studies conducted in the 1970–80s report inhibitory activities of nine different polyether ionophores against transmissible gastroenteritis (TGE), which is a corona virus that can infect the small intestine of pigs. Some of these agents were subsequently found to cure the infection in baby pigs (Liu, 1982). In 2014, evaluation of a panel of 290 drugs and drug candidates against MERS-CoV and SARS-CoV, revealed that 9 different ‘ion channel inhibitors’, including the polyether ionophores salinomycin and

* Corresponding author.

** Corresponding author.

E-mail addresses: holm@biomed.au.dk (C.K. Holm), thpou@chem.au.dk (T.B. Poulsen).

¹ These authors contributed equally.

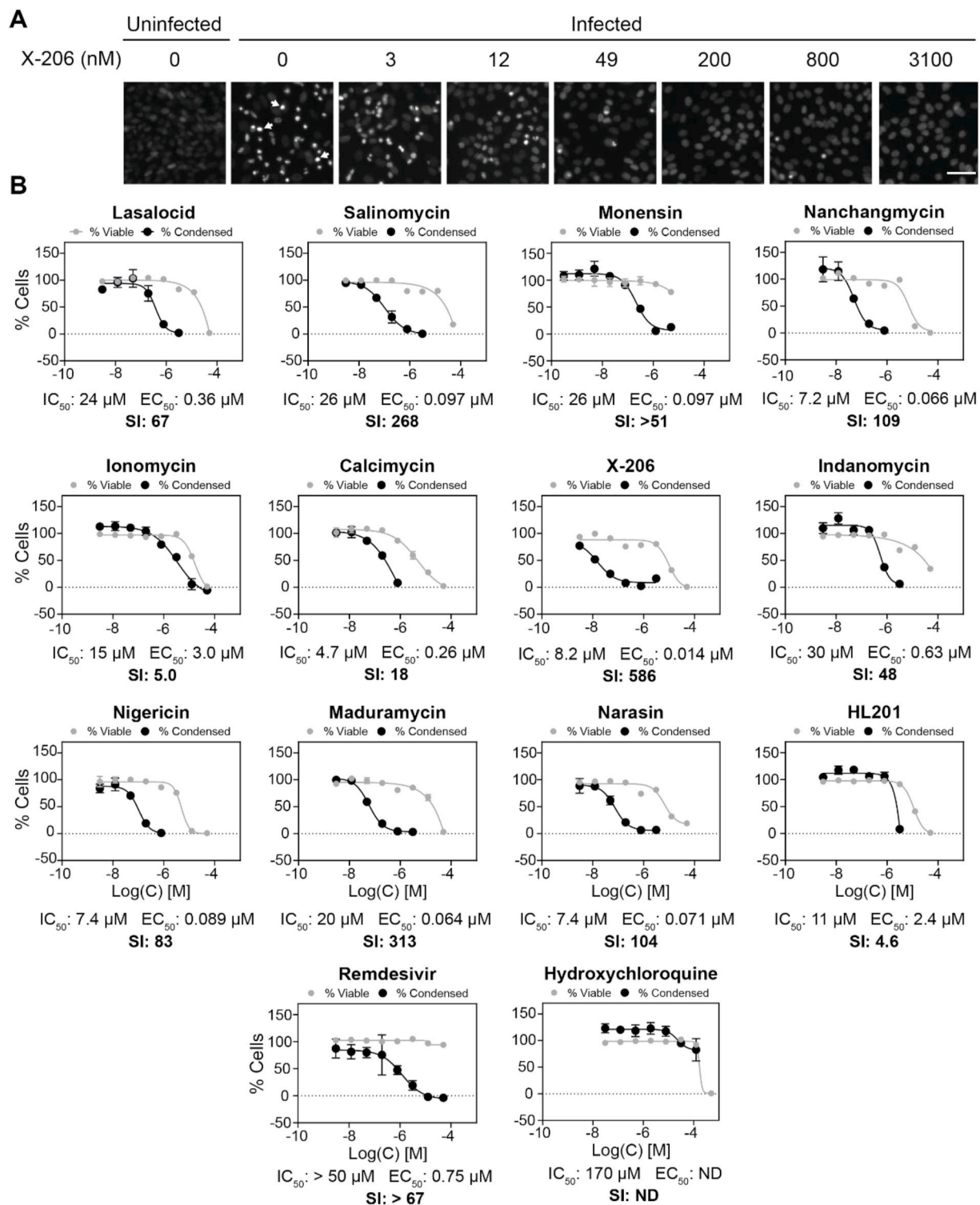


Fig. 1. Screen of polyether ionophores for antiviral activity against SARS-CoV-2 infection in Vero E6-hTMPRSS2 cells. (A) Representative microscope images. White arrows show examples of viral-induced condensed cells. Scale bar = 50 μm. (B) The relative number of viral-induced condensed cells (black lines) were counted and effects on cell viability of uninfected Vero E6-hTMPRSS2 cells were determined by CellTiter-Blue (grey lines). Data points are mean ± s.d. (N = 3). SI = selectivity index.

monensin, could inhibit the cytopathogenic effect of MERS-CoV, but not SARS-CoV. The specific potency and selectivity of the two molecules against MERS-CoV were however not reported (Dyall et al., 2014). The precise antiviral mechanism of the polyether ionophores is not currently known, and earlier studies indicate that the compounds can interfere with several steps in the viral replication cycle (Kevin II et al., 2009;

Jang et al., 2018; Rausch et al., 2017). Here, we conduct a focused investigation on a series of polyether ionophores for their ability to inhibit SARS-CoV-2 infection *in vitro*.

We conducted an initial screen of 11 different naturally occurring polyether ionophores and one synthetic analog (Fig. S1, Supplementary information) for their ability to rescue the cytopathogenic effect (CPE)

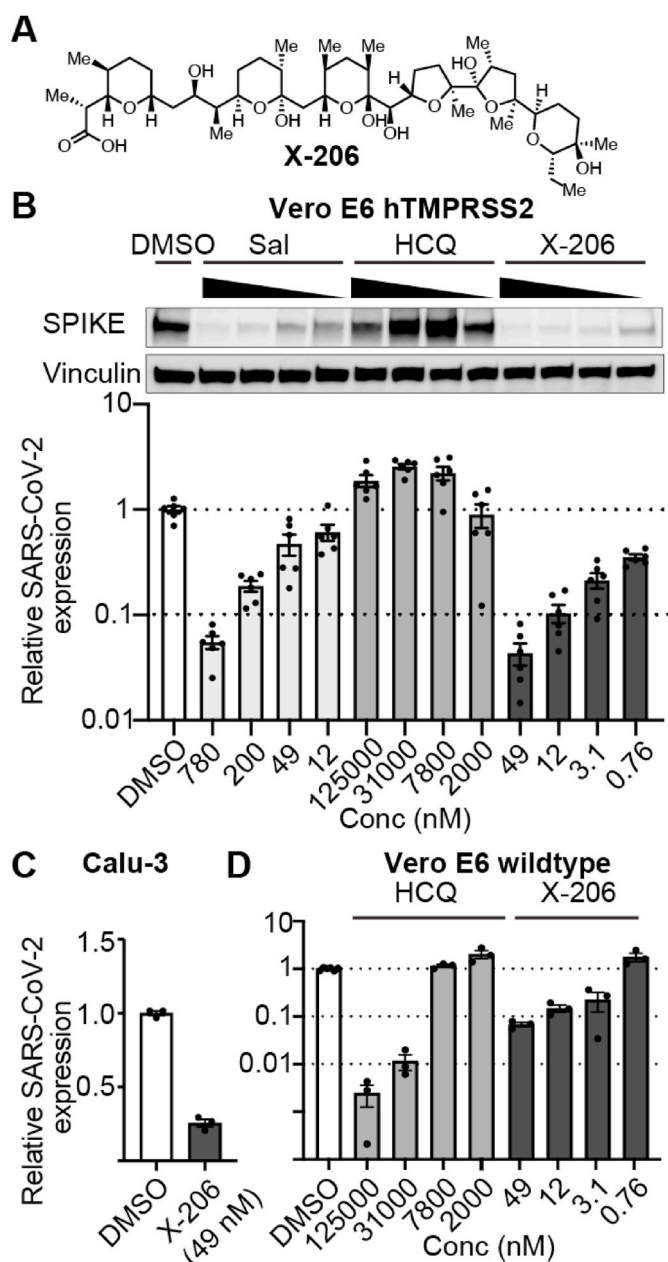


Fig. 2. Inhibitory potency of X-206 against SARS-CoV-2 replication. (A) Molecular structure of X-206. (B) Vero E6-hTMPRSS2 cells treated for 1 h followed by 24 h infection. Cells were harvested for Western blot and qPCR and tested for viral titer by Spike protein or SARS-CoV-2 RNA. Western blot is representative from an experiment repeated twice with consistent outcome. qPCR is mean \pm s. d., from two distinct experiments, conducted in triplicate. (C) Calu-3 cells were treated 1 h followed by 24 h infection. Cells were harvested for RNA extraction followed by qPCR for SARS-CoV-2 RNA. (D) Vero E6 wildtype cells were treated as in (B) and tested for viral titer by SARS-CoV-2 RNA. Data in (C) and (D) are mean \pm s.d. from an experiment conducted in triplicate. Sal = salinomycin, HCQ = hydroxychloroquine.

induced by SARS-CoV-2 viral infection of Vero E6 cells that overexpress the human serine protease TMPRSS2 (Vero E6-hTMPRSS2 cells). Remdesivir and hydroxychloroquine (HCQ) were used as controls. Viral infection produces a distinctive phenotype of high fluorescence cells with condensed chromatin that was quantified by microscopy (Fig. 1A). Interestingly, all 11 natural products display inhibitory activities in this assay although the potencies vary significantly as do the selectivity indices (SI) to effects on cellular viability (Fig. 1B). A subset, including

narasin, salinomycin, and nanchangmycin, display >100-fold selectivity while nigericin, indanomycin, monensin, and lasalocid have slightly lower selectivities (50–100 fold). By contrast, the canonical Cationophores ionomycin and calcimycin only show modest selectivity (5- and 18-fold). The synthetic polyether ionophore HL-201, despite having potent antibacterial activity (Lin et al., 2019), was unselective and scarcely active. We were, however, especially intrigued to also identify compounds with strongly enhanced selectivity windows and potency, maduramycin (EC_{50} = 64 nM, 313-fold selectivity), and, in particular, X-206 (EC_{50} = 14 nM, 586-fold selectivity). As expected, remdesivir displayed high selectivity (>67 fold, EC_{50} = 0.75 μ M), but hydroxychloroquine surprisingly had negligible anti-viral activity in this setting. We will return to the latter point below.

X-206 contains a series of unusual substructures including three lactol units (Fig. 2A) which, in solid-state structures, form direct interactions with bound metal ions (Blount and Westley, 1971). Interestingly, the compound was earlier found to also possess potent inhibitory activities against plasmodium parasites (Otoguro et al., 2001). To further substantiate the antiviral properties of X-206 against SARS-CoV-2, we next assessed the inhibitory potency of the compound against viral replication in Vero E6-hTMPRSS2 cells using dual readouts of qRT-PCR of viral RNA and formation of the SARS-CoV-2 spike protein (Fig. 2B). In this setting, X-206 displayed significant inhibition in both assays even at the lowest concentration tested (760 pM). In accord with the previous data (Fig. 1), salinomycin also showed potent inhibition. A standard plaque assay (Reinert et al., 2012) revealed that X-206 significantly reduced the release of infectious viral particles (Fig. S2, supplementary information). In addition, X-206 could also inhibit the replication of SARS-CoV-2 in Calu-3 human lung adenocarcinoma cells (Fig. 2C).

Cationic amphiphiles, including (hydroxy)chloroquine, are lysosomotropic agents that raise lysosomal pH and can e.g. block autophagic processes. These effects, on the host cells, are believed to, at least partially, underlie the inhibitory activities *in vitro* against several types of viruses observed with cationic amphiphiles (Salata et al., 2017). The use of (hydroxy)chloroquine for the clinical management of COVID-19 is, however, ineffective (Touret and de Lamballerie, 2020). As some polyether ionophores have also been reported to accumulate in lysosomes (Mai et al., 2017), to inhibit autophagy (Yue et al., 2013), and because their canonical activity to facilitate exchange of metal cations for protons could also alter lysosomal pH, it is possible that related mechanisms may underlie the antiviral activities of cationic amphiphiles and polyether ionophores. Given the above-mentioned limitations of cationic amphiphiles (Touret and de Lamballerie, 2020) this is a central question for the further evaluation of polyether ionophores as antivirals. In our initial screen, we found that hydroxychloroquine (HCQ) did not efficiently inhibit viral replication in Vero E6-hTMPRSS2 cells (Fig. 2B), but the compound was effective in wildtype Vero E6 cells at high micromolar concentrations in accord with data in the literature (Liu, 2020) (Fig. 2D). In comparison, the potent (low nanomolar) antiviral activity of X-206 was not dependent on hTMPRSS2 expression which suggests a mechanistic difference in this experimental setting (Fig. 2B, D). To further provide an initial unbiased mechanistic comparison, we also used morphological profiling (Bray et al., 2016) to compare the effects of both types of compounds on Vero E6-hTMPRSS2 cells in the absence of viral infection (Fig. 3A and B). Similar to standard transcriptional profiling, morphological profiling can provide bioactivity fingerprints of small molecules, which can be used statistically to compare their mechanistic similarities (Svenningsen and Poulsen, 2019). Hydroxychloroquine (HCQ), DC661, which is also a cationic amphiphile, and bafilomycin, a natural product inhibitor of V-ATPase with antiviral activity (Yeganeh et al., 2015), all have highly correlated (Pearson correlation coefficient $P > 0.7$) bioactivity profiles, suggesting a shared cellular mechanism which is likely driven by lysosomal deacidification (Fig. 3A,B, Fig. S3, Supplementary information). In contrast, a selected subset of the polyether ionophores afforded

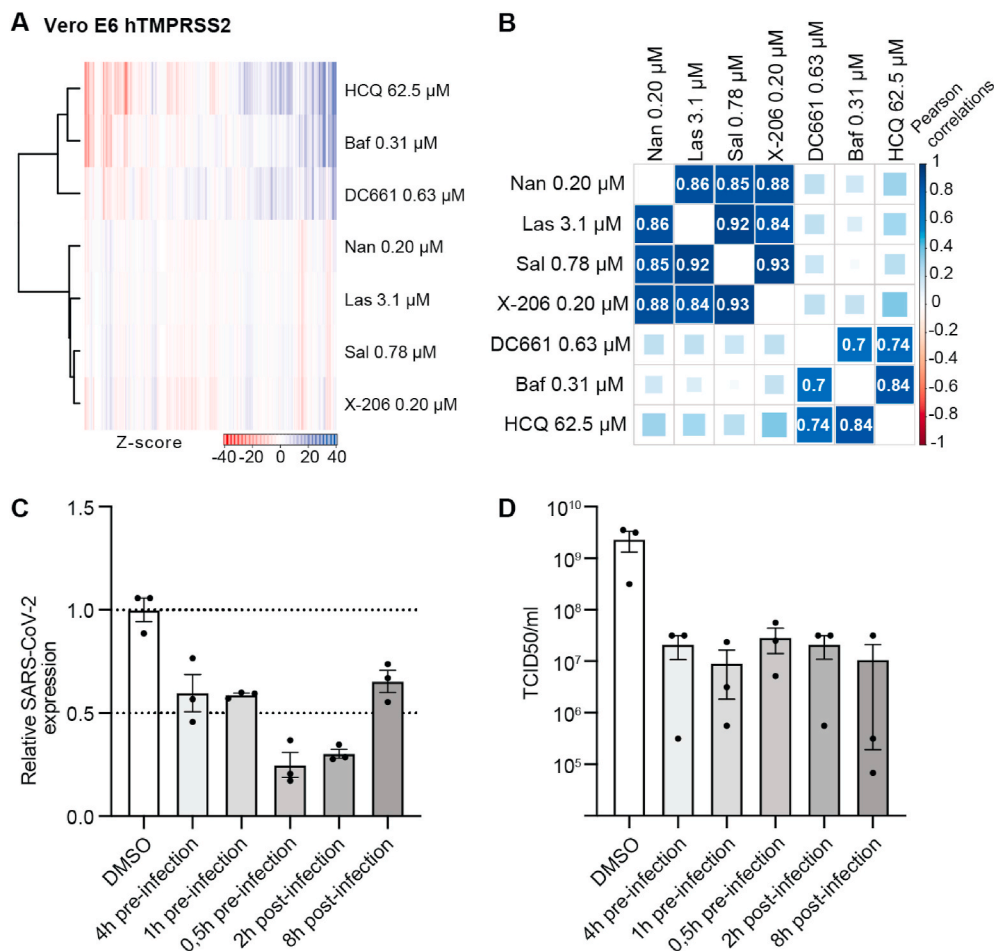


Fig. 3. Comparison of polyether ionophores with cationic amphiphiles and time-dependence of the anti-viral activity of X-206. (A) The Z-scored averaged bioactivity profiles for morphological profiling of selected polyether ionophores and cationic amphiphiles. (B) Pearson correlation matrix of profiles ordered by hierarchical clustering. Polyether ionophores and cationic amphiphiles show different mechanistic fingerprints. (C,D) Time-dependence of the ability of X-206 (12 nM) to reduce viral titers as measured by qPCR for SARS-CoV-2 RNA (C) and to suppress release of infectious viral particles to the supernatant (D). Data in (C) and (D) are mean \pm s.d. from an experiment conducted in triplicate. Nan = nanchangmycin, Las = lasalocid acid, Sal = salinomycin, Baf = bafilomycin, HCQ = hydroxychloroquine.

bioactivity profiles that were clearly distinct from those of the cationic amphiphiles and bafilomycin, but strongly internally correlated ($P > 0.8$). The same clustering of compounds was observed in wildtype Vero E6 cells (Fig. S4, Supplementary information). The bioactive concentrations of the respective polyether ionophores in the morphological profiling assay roughly correlated with their antiviral concentrations. This experiment suggest that polyether ionophores mediate their antiviral effects through a mechanism that is different from that of the lysosomotropic, cationic amphiphiles. Finally, we conducted a time-of-addition experiment to study the effectiveness of X-206 for suppressing viral replication depending on the relative timing of compound exposure and viral challenge. X-206 (12 nM) was effective at all time points with the most significant reduction in viral mRNA (measured 24 h after infection) observed at either 0.5 h pre-infection or 2 h post-infection (Fig. 3C). We also measured the TCID₅₀/mL (Olagnier et al., 2020) which demonstrated a nearly 2-fold log-reduction of infectious viral progeny in the supernatant at all time points (Fig. 3D).

The human safety data for polyether ionophores is – to the best of our knowledge – not known and these compounds, including X-206, have toxicity in some animals (Liu, 1982). However, some members are used – safely – in the agricultural industry, and thus produced industrially, which makes them relevant to consider for further studies. Our current data confirms the broad-spectrum antiviral activities of polyether ionophores, including salinomycin (Jeon, 2020), monensin and lasalocid, also against pandemic SARS-CoV-2, and furthermore reveals X-206 as a family member of highly notable potency and selectivity. Future studies will be aimed on understanding the underlying antiviral mechanism which may also shed light on the potential for further pre-clinical development.

Acknowledgments

This project has received funding from the European Research Council (ERC) under the European Union's Horizon 2020 research and innovation programme (grant agreement No 865738). The project was also supported by Independent Research Fund Denmark (grants 9040-00117B, 0214-00001B, 9039-00078B), the Carlsbergfoundation (grant CF17-0800), Ester M og Konrad Kristian Sigurdssons Dyreværnsfond, Beckett-Fonden, Kong Christian IX og Dronning Louises Jubilæumslegat, Læge Sofus Carl Emil Friis og Hustru Olga Doris Friis' legat, Købmand I Odense Johan og Hanne Weimann Født Seedorffs Legat, and Lundbeck foundation.

Appendix A. Supplementary data

Supplementary data to this article can be found online at <https://doi.org/10.1016/j.antiviral.2020.104988>.

References

- Blount, F., Westley, J.W.J., 1971. X-Ray crystal and molecular structure of antibiotic X-206. *J. Chem. Soc. D Chem. Commun.* 927–928.
- Bray, M.-A., et al., 2016. Cell painting, a high-content image-based assay for morphological profiling using multiplexed fluorescent dyes. *Nat. Protoc.* 11, 1757–1774.
- Caly, L., Druce, J.D., Catton, M.G., Jans, D.A., Wagstaff, K.M., 2020. The FDA-approved drug ivermectin inhibits the replication of SARS-CoV-2 in vitro. *Antivir. Res.* 178, 104787.
- Chapman, H.D., Jeffers, T.K., Williams, R.B., 2010. Forty years of monensin for the control of coccidiosis in poultry. *Poultry Sci.* 89, 1788–1801.
- Choy, K.-T., et al., 2020. Remdesivir, lopinavir, emetine, and homoharringtonine inhibit SARS-CoV-2 replication in vitro. *Antivir. Res.* 178, 104786.

- Dyall, J., et al., 2014. Repurposing of clinically developed drugs for treatment of Middle East respiratory syndrome coronavirus infection. *Antimicrob. Agents Chemother.* 58, 4885–4893.
- Jang, Y., et al., 2018. Salinomycin inhibits influenza virus infection by disrupting endosomal acidification and viral matrix protein 2 function. *J. Virol.* 92 e01441–18.
- Jeon, S., et al., 2020. Identification of antiviral drug candidates against SARS-CoV-2 from FDA-approved drugs. *Antimicrob. Agents Chemother.* 64, e00819–20.
- Kevin II, D.A., Meujo, D.A., Hamann, M.T., 2009. Polyether ionophores: broad-spectrum and promising biologically active molecules for the control of drug-resistant bacteria and parasites. *Expert Opin. Drug Discov.* 4, 109–146.
- Lin, S., et al., 2019. Diversity focused semisyntheses of tetronate polyether ionophores. <https://doi.org/10.26434/chemrxiv.8299715>. (Accessed 13 June 2020).
- Liu, C.-M., 1982. Microbial aspects of polyether antibiotics: activity, production, and biosynthesis. In: Westley, J.W. (Ed.), *Polyether Antibiotics - Naturally Occurring Acid Ionophores Biology*, vol. 1. Marcel Dekker, pp. 50–51.
- Liu, J., et al., 2020. Hydroxychloroquine, a less toxic derivative of chloroquine, is effective in inhibiting SARS-CoV-2 infection in vitro. *Cell Discov.* 6, 16.
- Mai, T.T., et al., 2017. Salinomycin kills cancer stem cells by sequestering iron in lysosomes. *Nat. Chem.* 9, 1025–1033.
- Nakamura, M., et al., 1992. Inhibitory effects of polyethers on human immunodeficiency virus replication. *Antimicrob. Agents Chemother.* 36, 492–494.
- Olagnier, D.P., et al., 2020. Identification of SARS-CoV-2-mediated suppression of NRF2 signaling reveals a potent antiviral and anti-inflammatory activity of 4-octyl-itaconate and dimethyl fumarate. *Nat. Commun.* 11, 4938.
- Otoguro, K., et al., 2001. Potent antimalarial activities of polyether antibiotic, X-206. *J. Antibiot.* 54, 658–663.
- Rausch, K., et al., 2017. Screening bioactives reveals nanchangmycin as a broad spectrum antiviral active against zika virus. *Cell Rep.* 18, 804–815.
- Recovery Collaborative Group, et al., 2020. Dexamethasone in hospitalized patients with Covid-19 - preliminary report. *N. Engl. J. Med.* <https://doi.org/10.1056/NEJMoa2021436>.
- Reinert, L.S., et al., 2012. TLR3 deficiency renders astrocytes permissive to herpes simplex virus infection and facilitates establishment of CNS infection in mice. *J. Clin. Invest.* 122, 1368–1376.
- Rutkowski, J., Brzezinski, B., 2013. Structures and properties of naturally occurring polyether antibiotics. *BioMed Res. Int.* 2013, 162513.
- Salata, C., et al., 2017. Antiviral activity of cationic amphiphilic drugs. *Expert Rev. Anti Infect. Ther.* 15, 483–492.
- Svenningsen, E.B., Poulsen, T.B., 2019. Establishing cell painting in a smaller chemical biology lab – a report from the frontier. *Bioorg. Med. Chem.* 27, 2609–2615.
- Touret, F., et al., 2020. In vitro screening of a FDA approved chemical library reveals potential inhibitors of SARS-CoV-2 replication. *Sci. Rep.* 10, 13093.
- Touret, F., de Lamballerie, X., 2020. Of chloroquine and COVID-19. *Antivir. Res.* 177, 104762.
- Wu, F., et al., 2020. A new coronavirus associated with human respiratory disease in China. *Nature* 579, 265–269.
- Yeganeh, B., et al., 2015. Suppression of influenza A virus replication in human lung epithelial cells by noncytotoxic concentrations bafilomycin A1. *Am. J. Physiol. Lung Cell Mol. Physiol.* 308, L270–L286.
- Yue, W., et al., 2013. Inhibition of the autophagic flux by salinomycin in breast cancer stem-like/progenitor cells interferes with their maintenance. *Autophagy* 9, 714–729.
- Zhu, N., et al., 2020. A novel coronavirus from patients with pneumonia in China, 2019. *N. Engl. J. Med.* 382, 727–733.